BASIC DEFORMATIONS OF HIGH-PERFORMANCE CONCRETE

Bertil Persson, M.Sc., Lic. Tech., CIV.ENG.
Lund Institute of Technology, Division of Building Materials, Lund University, P O Box 118, 221 00 Lund, Sweden

ABSTRACT

Creep and shrinkage are two major problems to be discussed in concrete design. Basic creep is studied during constant loading, temperature and moisture conditions, i.e. no exchange of moisture takes place to or from the specimen during the test period. In this paper an experimental and numerical study of basic creep of High-Performance Concrete (HPC) is outlined. For this purpose cylinders and cubes were cast. Quasi-instantaneous deformation and basic creep including autogenous shrinkage were observed over 3 years. Analysises of elastic modulus, early creep and long-term creep including autogenous shrinkage are presented. HPC autogenous shrinkage had a great influence on the results. The autogenous shrinkage in its turn is caused by the self-desiccation of HPC. The study was carried out in 1992 through 1994 at Lund Institute of Technology, Division of Building Materials, Lund, Sweden.

Keywords: Autogenous shrinkage, Basic creep, Basic deformations, Creep, Creep rate, Elastic modulus.

1. INTRODUCTION

1.1 Background

The fundamental cause of creep is still unknown. Moisture movement in the gel of HPC is one probable cause of creep. Creep and shrinkage influence the properties of the young concrete as well as the long-term behaviour of the concrete, i.e. deformations, stability and durability. Basic deformations of HPC are not only related to imposed loading on the concrete. HPC deforms with sealed curing as well, free of imposed stresses (autogenous shrinkage). HPC exhibits autogenous shrinkage under sealed conditions until it cracks. At low imposed loading the HPC creeps as long as the self-desiccation continues. Problems related to creep are especially pronounced when the concrete is used in prestressed structures. If the prestressing is done at one side of the structure, the result is often a bent element caused by creep due to the prestressing. One of the great advantages of HPC seems to be low creep and shrinkage as compared with normal concrete. The assumed advantages of HPC remain to be confirmed.

1.2 Purpose of the study

One purpose of the study was to ascertain the amount of elastic deformation and basic creep of HPC with water-cement ratio, w/c, varying between 0.25 and 0.38. The effect of hydration on

the creep properties was secured studying both mature and young HPC. Another purpose was to ascertain a relationship between creep rate, $\delta\varepsilon/\delta t$, and strength growth rate, $\delta f_c/\delta t$, according to the hypothesis:

$$d\varepsilon/dt = k \cdot \delta f_c/\delta t \quad (1)$$

A third purpose of the study was to ascertain a model of autogenous shrinkage by studying HPC with w/c varying between 0.25 and 0.38 parallel with studies of the internal relative humidity of the concrete for at least 2 years. The effect of air-entrainment and of different amounts of silica fume additive was to be ascertained at one w/c only.

1.3 General layout of the work

Studies of separation of elastic deformation from plastic and viscous creep were carried out on cylinders in an oil accumulator and electronic servo-controlled machine (MTS). The deformations were measured by separate displacement and gauging transducers (LVDT) collected by a separate computer. The full level of loading was applied within 0.01 s. At loading and unloading the measurements were carried out about 1000 times per second including 3 longitudinal LVDTs and one LVDT placed transversally to the cylinder. The work was principally according to /1/ and /2/. Autogenous shrinkage had a great influence on the result /3, 4, 5/. Studies of autogenous shrinkage were carried out on horizontal (lying) cylinders. The cylinders were turned a third of a full turn at each measurement to avoid bending effects. The weight of the cylinder was continuously established. The autogenous shrinkage in its turn was caused by the self-desiccation of HPC /6/. An internal relative humidity as low as 0.72 was observed in HPC /7/. The pronounced self-desiccation also had an influence on the strength and hydration of HPC /8/. Long-term creep tests were carried out for 3 years on cylinders in a traditional mechanical spring loading device. During all measurements the specified loading of the spring was applied. The loading of the spring device was applied simultaneously to the loading in the MTS machine. Thus the quasi-instantaneous loading in the MTS machine was prolonged by studies of creep in the traditional spring device. The weight of the cylinders was established before and after the long-term studies.

2. MATERIALS, TESTED CONCRETES

The HPCs had good rheological properties and a 28-day 100 mm cube compressive strength exceeding 80 MPa. In a fresh state it was possible to mix, transport and cast HPC with existing methods. The w/c varied between 0.25 and 0.38. A low-alkali cement, Cementa Degerhamn Standard, was used. Appendix 1 gives the chemical composition of the cement /9/. Eight types of concrete were studied, 16 cylinders of each quality, in all 128 concrete cylinders. Properties of the aggregate are given in Appendix 2 /9, 10/. Appendix 3 shows the mix design of the concretes. Different types of aggregate were used since the study was a part of an international programme on HPC, in which different properties of HPC were compared with the mix design held constant. However, the chosen types of aggregate did not exhibit creep itself and did not affect the result of the study. The aggregate content varied slightly between the HPCs, Appendix 3, mainly due to the reason mentioned above. It also varied between the mix designs due to recalculations that were performed after the mixing of the concrete when the density was known. This article will show that small variations in the aggregate content did not affect creep properties of HPC.

3. SPECIMENS AND CURING CONDITIONS

Basic creep and autogenous shrinkage of HPC were studied for cylinders 300 mm long with a diameter of 55 mm. Other properties of the concrete such as compressive strength and internal relative humidity were studied on 100 mm cubes. A constant temperature of 20°C ±1°C during the test period was obtained in a climate chamber. The specimens were sealed from moisture by insulation with 2 mm rubber covering (the weight of a cylinder, 1.8 kg, dropped only about 1 g over 1 year). The moisture absorption of the rubber was about 0.2 g as measured on one specimen.

4. EXPERIMENTAL METHODS

4.1 Short-term creep

Short-term creep was studied in an oil accumulator and electronic servo-controlled machine (MTS) for 66 h. The loading was applied within about 0.01 s. A method of rapid loading and simultaneous registration of measurements was developed. The age of the concrete was 1, 2 or 28 days at the commencement of testing. At 1 and 2 days' age a stress/strength ratio of 0.6 was used; at 2 and 28 days the ratio was 0.3. The rapid loading gave the possibility of estimating the initial strain (true modulus of elasticity) and very early creep. This was of great interest for prestressed structures and also for studies of the effect of creep during hydration. After the rapid (quasi-instantaneous) loading of the cylinders, the deformations were continuously studied over a period of 66 hours. The unloading of the cylinders was then carried out within 1 s. The recovery was studied for 100 hundred hours. At this time most of the recovery seemed to be finished except for the mature concrete. The measurements were performed by gauging and displacement transducers (LVDT). The longitudinal deformation was measured along three sides of the specimen, which gave the possibility to calculate the eccentricity of the loading. Transversal measurements gave the resulting Poisson's ratio.

4.2 Long-term creep

The long-term creep was studied in traditional spring-loading devices by applying the loading at a rate of 1 MPa/s. The long-term creep was studied for at least 1 year. The long-term loading on 32 cylinders in spring-loading devices was applied parallel to the rapid loading in the MTS machine the same time (and at the same age) of the concrete. Twenty concrete cylinders of 5 concretes studied in the spring-loading devices were unloaded after at least 1 year of creep deformation. Mechanical devices were used to obtain measurements of the long-term deformations to avoid errors due to creep of the measurement device itself. Also these deformations were measured along three sides of the specimen.

4.3 Shrinkage

Self-desiccation of HPC caused autogenous shrinkage, an unfavourable property of HPC. Self-desiccation and consequently also autogenous shrinkage may occur even under wet conditions due to the low permeability of HPC /7/. The autogenous shrinkage was measured on 32 cylinders of the same type as used in the creep tests. The temperature development due to hydration (increase of 4°C within 16 h age) was measured by cast-in thermo couples to avoid faults due to temperature movements. The specimens were weighed to control the moisture

losses. The deformation was measured along three sides of the specimen. Compressive cylinder strength was studied on 32 cylinders. The cube strength was measured on about 400 cubes (100 mm) from 0.8 until about 1000 days' age. Directly after the compressive strength tests were performed, fragments of the concrete (minimum 10 mm in size) were collected in 100 ml glass test tubes. The tubes were filled up to 2/3. They were then sealed with rubber plugs. The tubes with the fragments were kept in a 20°C ± 1°C climate room. A dew point meter was used to measure the internal relative humidity, Ø. The dew point meters were calibrated monthly /11/. The probe of the dew point meter was entered into the test tube and rubber-sealed to the glass by an expanding ring. Since HPC contains very little moisture, the required period of measurement to obtain a stable value of Ø was at least 12 hours. The minimum period was thus set at 16 hours.

5. RESULTS OF BASIC CREEP STUDIES

It was appropriate to describe the basic deformation related to a unit stress (ε/σ), a parameter called compliance, J(t,t') /12/. Figure 1 shows the very early compliance of HPC type 31g10, Appendix 3. In all 8 tests were carried out at each age. The measurements of the tests exhibited very high accuracy. The differences in compliance due to the maturity of the concrete were remarkably high. The creep of a young concrete (0.8 days' age) was more than twice as much as that of an old concrete at the same stress/strength ratio. At the same age, 2 days, there also was some influence of the stress/strength ratio on the size of the creep. By applying 60% of the ultimate strength instead of 30%, the creep became larger within the 66 hours of loading. Figure 2 shows the long-term compliance (σ/ε) of HPC 31g10, Appendix 3. Symbols:

f_c denotes current cube strength (MPa)
σ denotes the stress in the concrete (MPa)
1 denotes loading at 0.8 days' age; σ/f_c=0.6
2 denotes loading at 2 days' age; σ/f_c=0.6
3 denotes loading at 2 days' age; σ/f_c=0.3
28 denotes loading at 28 days' age; σ/f_c=0.3.

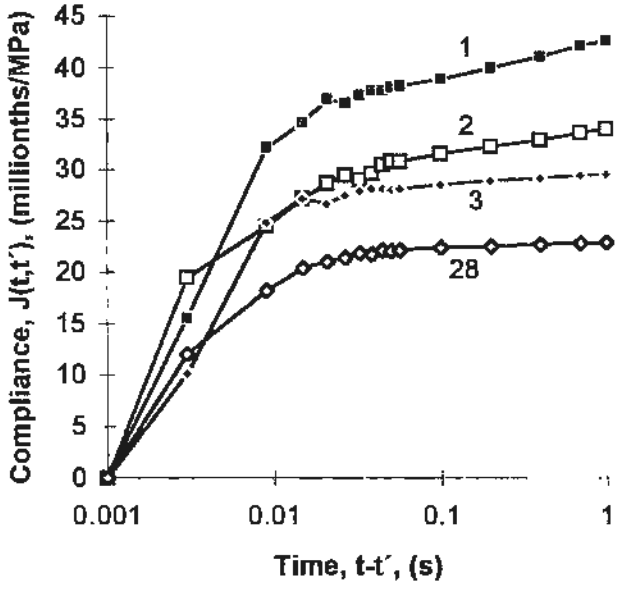

Figure 1. Early compliance of HPC 31g10.

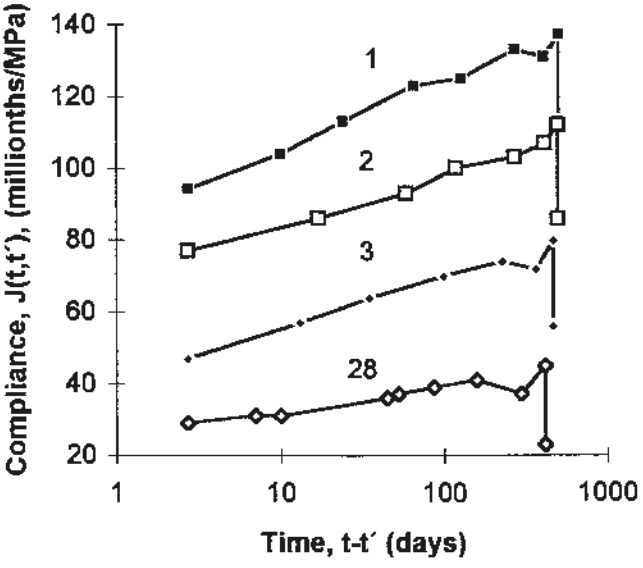

Figure 2. Long-term compliance of HPC 31g10.

The compliance of short-term and long-term creep tests coincided well after 66 h of creep. The unloading of the cylinders, shown in Figure 2, was carried out within 1 s after a loading period of 66 hours. The remaining compliance was then observed by rapid measuring. The remaining compliance increased slightly as the w/c increased. The ageing effect was, however, much larger. A young concrete during hydration obtained much larger creep deformation than a mature concrete. The recovery compliance for a mature concrete (28 days' age) was fairly independent of the w/c. As the stress applied to the concrete increases at a decreased w/c, the actual recovery strain also increases at a decreased w/c, i.e. at higher strength. The size of the plastic creep (remaining creep) of a concrete loaded at early ages was clearly related to the maturity at loading. HPC with 10% silica fume showed smaller long-term creep rate than HPC with 5% silica fume. However, HPCs that were loaded at early ages exhibited larger long-term creep rate than HPCs that were mature at loading. Figure 3 shows the long-term compliance.

6. RESULTS OF ELASTIC MODULUS AND AUTOGENOUS SHRINKAGE

The elastic recovery strain after unloading was more or less identical to the same property after the short-term tests, i.e. the modulus of elasticity was related to the strength /13/. A quite large portion of the basic creep of an HPC was related to the autogenous shrinkage, especially when the concrete was loaded at early ages. Figure 4 shows autogenous shrinkage versus the internal relative humidity, Ø. The autogenous shrinkage was found to be larger in relation to Ø at 10% silica fume in the concrete than at 5% silica fume due to the pronounced self-desiccation.

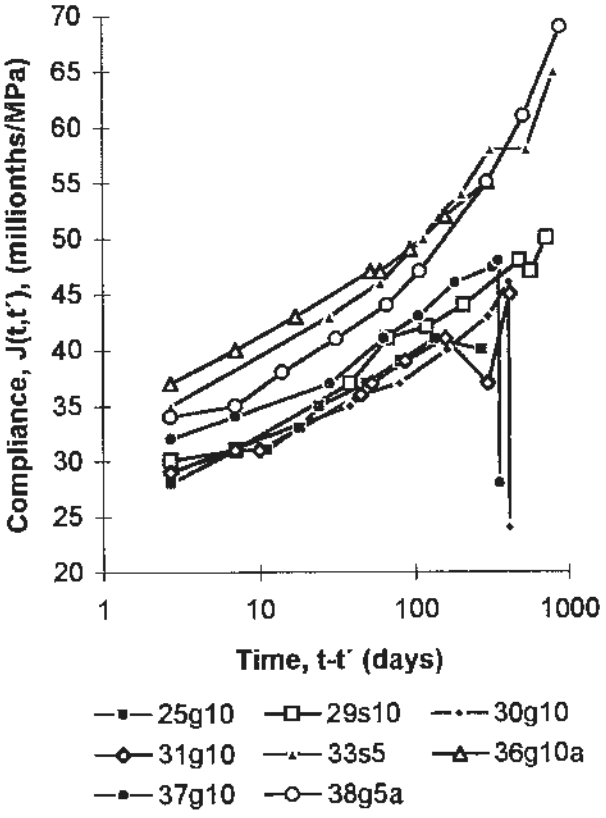

Figure 3. Long-term compliance of HPCs that were mature at loading. Mix design: Appendix 2.

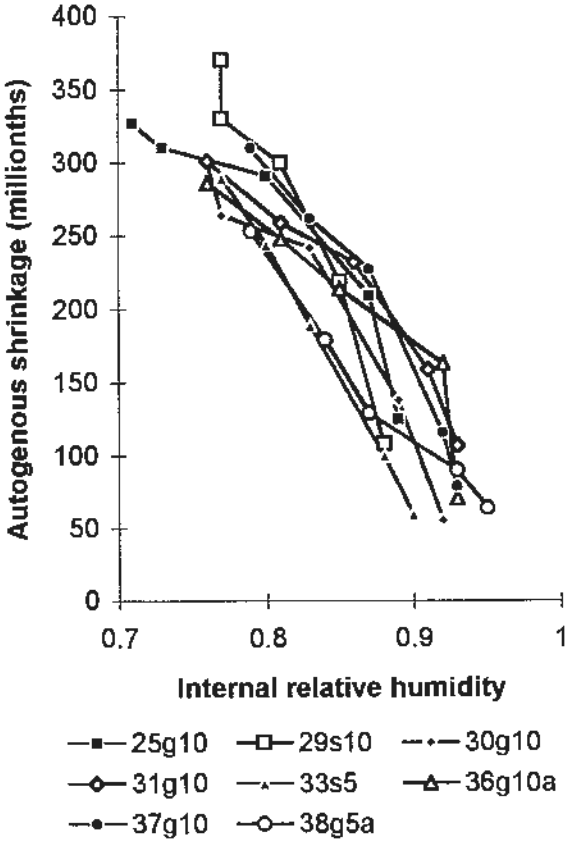

Figure 4. Autogenous after 2 years versus internal relative humidity.

7. ANALYSES OF BASIC CREEP

As indicated above, the knowledge of the long-term basic creep rate was of the utmost importance for the lifetime of a concrete structure. Present codes often underestimate the effect of the creep, most probably due to low creep rate assumption /14/. As proposed /12/, the basic creep may be separated into one part related to creep and another part consisting of the initial deformations. Therefore it was essential to describe the slope of the creep function, i.e. the creep rate. From the eight long-term creep tests carried out within the project the long-term creep rate, $\partial C_0(t,28)/\partial t$, for mature concrete was expressed in relation to the 28-day strength (millionths/(MPa·day)) / 9/:

$$\frac{\partial C_0(t,28)}{\partial t} = k \cdot 0.25 \cdot (f_{c28})^{-0.84} \cdot (t-28)^{k\cdot(0.19\cdot f_{c28}-0.81)} \quad \{R^2=0.83\} \qquad (2)$$

$$R^2 = 1 - \frac{\sum (Y_i - Y_m)^2}{(\sum Y_i^2) - \frac{(\sum Y_i)^2}{n}} \qquad (3)$$

f_{c28} denotes 28-day cube strength (N.B.: GPa); {0.085< f_{c28}<0.145 GPa cube strength}
k k= 1 at 10% silica fume; k≈ 0.92 at 5% silica fume
n denotes the number of measured values
t denotes the age (days); {28<t<720 days}
Y_i denotes the measured value
Y_m denotes the average measured value

The long-term creep rate of concrete, young at loading, $\partial C(t,t')/\partial t$, varied mainly with the relative 28-day strength of the concrete. In this case, 24 tests of HPC were available for analysis. The long-term term studies indicated that, even after long time, the creep rate of a concrete, young at loading, was higher than that of a concrete that was mature at loading. The creep rate was expressed as (millionths/(MPa·day)) /9/:

$$\frac{\partial C(t,t')}{\partial t} = 11 \cdot e^{-2\cdot\varpi} \cdot (t-t')^{0.95\cdot f_{c28}\cdot(\ln\varpi - 0.54)-0.72} \quad \{R^2=0.93\} \qquad (4)$$

f_c denotes the cube strength at loading (N.B.: GPa)
f_{c28} denotes the cube strength at 28 days' age (N.B.: GPa); {0.085< f_{c28}<0.145 GPa }
t denotes the age (days); { 2<t<720 days}
t′ denotes the age at loading (t> t′) (days); limits: {0.8<t′<3days}
R^2 denotes a parameter given above
ϖ =$f_c/(f_{c28})$; {0.15<ϖ<0.65}

8. ANALYSES OF ELASTICITY AND AUTOGENOUS SHRINKAGE

The modulus of elasticity was obtained when unloading 20 cylinders after 1 year of loading. The deformation modulus was obtained at loading times of 0.01 s, 0.1 s and 1 s. The elastic modulus when unloading was related to the deformation modulus at rapid loading about 0.01 s after loading. Figure 5 shows the elastic modulus versus the cube strength, /9, 14, 15/. The following correlation applied between the strength and the elastic modulus, E_t (GPa, /9/):

$$E_t=0.435\cdot[(7.88 - \ln(t)]\cdot(f_c)^{0.168\cdot(3.13 + 0.1\cdot\ln t)} \qquad \{R^2=0.92\} \qquad (5)$$

f_c denotes the 100 mm cube strength (MPa); $\{8< f_c<145$ MPa$\}$
t denotes the time from loading to measuring (s); $\{0.01<t<1$ s$\}$
R^2 denotes a parameter given above

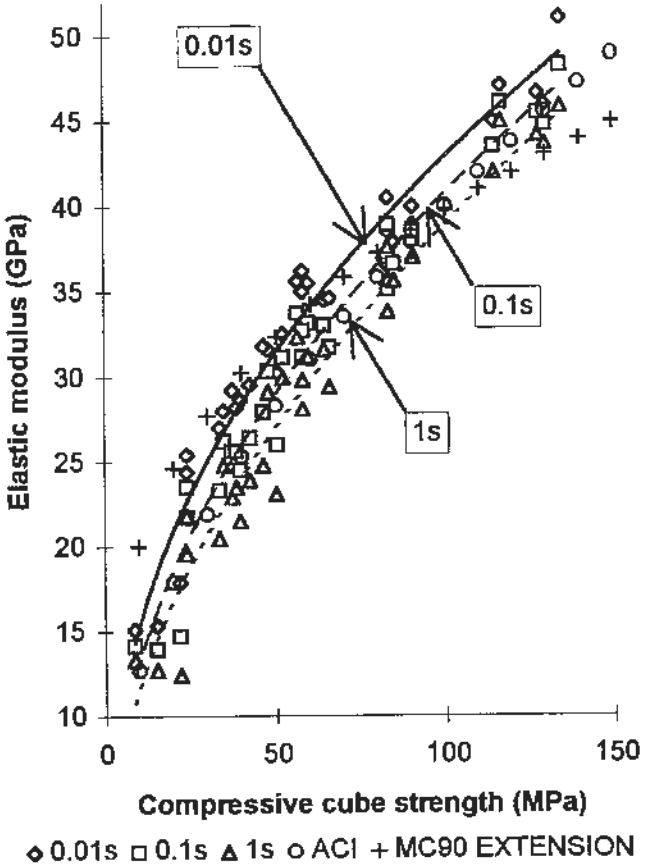

Figure 5. Elastic modulus versus cube strength at varying time of measurement.

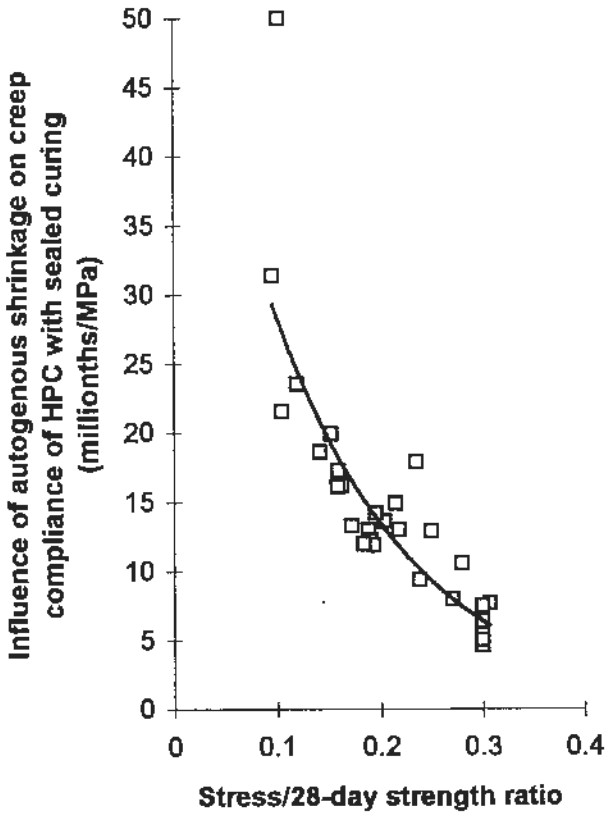

Figure 6. Effect of autogenous shrinkage on basic creep after 2 years versus the w/c.

The results of the studies of the elastic modulus coincided reasonably well with /15/ with some divergence to /16/. At high strength Eq. (4) overestimated the elastic modulus, probably due to the moisture conditions in the specimen. Specimens with sealed curing exhibit a larger immobility of water transports in the structure than drying specimens with partly emptied pores. The autogenous shrinkage was related to the internal relative humidity, Figure 4:

$$\varepsilon_{bs}\approx 1320\cdot(0.98-Ø) \qquad \{0.80<Ø<0.96\} \qquad \{R^2=0.93\} \qquad (6)$$

$\varepsilon_{br} \approx 170 \cdot \ln(1-Ø) + 550$ {0.72<Ø<0.94} {R^2=0.91} (7)

$\varepsilon_{bR} \approx 350 \cdot \ln(1-Ø) + 860$ {0.77<Ø<0.88} {R^2=0.95} (8)

R^2 denotes a parameter given above
ε_{b5} denotes the autogenous shrinkage for HPC containing 5% silica fume (millionths)
ε_{br} denotes autogenous shrinkage for HPC with 10% granulated silica fume (millionths)
ε_{bR} denotes autogenous shrinkage for HPC with 10% silica fume slurry (millionths)
Ø denotes the internal relative humidity

The internal relative humidity, Ø, was measured as specified above and correlated to age, content and type of silica fume and w/c /9/:

$Ø(wbr_{eff}, t) = 0.38 \cdot (wbr_{eff} + 2.4 - 0.1 \cdot \ln t) - Ø_{sl}$ {R^2=0.83} (9)

$wbr_{eff} = w/(c+2 \cdot s)$ (10)

c denotes the cement content in the concrete (kg/m^3)
s denotes the content of silica fume in the concrete (kg/m^3)
t denotes the age of the concrete {1<t<1000 days}
w denotes the water content in the concrete (kg/m^3)
R^2 denotes a parameter given above
$Ø_{sl}$ = -0.035 for silica fume slurry when t<28 days

The effect of the fineness of the silica fume on the internal relative humidity was also observed by others /17/. The rate of self-desiccation was calculated by derivation of Eq. (9) (day^{-1}):

$\delta Ø/\delta t = 0.038/t$ (11)

The rate of self-desiccation thus was a logarithmic constant related to the age of HPC. The affect of autogenous shrinkage on the basic creep (assuming the principle of superposition) was small on HPC that was mature at loading. Figure 6 shows the effect of autogenous shrinkage on compliance when the loading was applied at early ages. At 2 years' age the effect varied between 5 and 50 millionths/MPa. The following correlation was obtained for the effect of autogenous shrinkage on compliance, $\Delta J(t, t', \omega)$, (millionths/ MPa) /9/:

$\Delta J(t, t', \omega) = 9.2 \cdot e^{-7.4 \cdot \omega} \ln(t-t')$ {R^2=0.79} (12)

f_{c28} denotes the 28-day strength (MPa)
t denotes the age of the concrete (days)
t′ denotes the age at loading (days)
R^2 denotes a parameter given above

$\Delta J(t, t', \omega)$= denotes effect of autogenous shrinkage on total compliance (millionths/ MPa)
σ denotes the stress applied (MPa)
ω= σ/f_{c28}; {0.1<ω<0.3}

9. DISCUSSIONS

Eqs. (2) and (4) were compared with a creep rate model named B_3 /12/ using the concretes in the study (Appendix 3). Model B_3 /12/ was simplified and transformed as follows /18/:

$$\frac{\partial C_0(t,t')}{\partial t} = \frac{45.11 \cdot \sqrt{c} \cdot \left[1/\sqrt{t} + 0.29 \cdot (w/c)^4\right]}{(f'_c)^{0.9} \cdot \left[(t-t') + (t-t')^{0.9}\right]} + \frac{0.14}{t \cdot (a/c)^{0.7}} \qquad (13)$$

a denotes the aggregate content (lb/ft^3)
c denotes the cement content in the concrete (lb/ft^3)
f'_c denotes the cylinder strength (psi)
t denotes the age of the concrete (days)
t′ denotes the age at loading (days)
w denotes the water content at mixing (lb/ft^3)
$\delta C_0/\delta t$ denotes the creep rate of the concrete (millionths/(psi·day))

In the comparisons a stress to strength ratio at loading of the concrete, $\sigma/f_c = 0.3$ (based on the cube strength, f_c) was studied. Both young concrete (2 days' age) and mature concrete (28 days' age) were used in the comparison. Model B_3 applied for $\sigma/f'_c < 0.4$ (cylinder strength, f'_c). Cylinder strength, f'_c, of 32 cylinders was correlated to cube strength, f_c, Figure 7 (MPa):

$$f'_c = 0.73 \cdot f_c \qquad \{R^2 = 0.94\} \qquad (14)$$

The stress/cylinder strength ratio at loading of the specimens in the study was then calculated: $\sigma/f'_c = 0.41$. Figure 8 shows the creep rate estimated according to Eqs. (2) and (4) /9/ and according to Eqs. (13) /12/ and (14) versus the measured creep rate in the present study /9/.

The precise estimations according to Eq. (13) are given in Appendix 4. The estimations according to Eq. (13) gave a decreasing creep rate with increasing compressive strength, which was contrary to Eqs. (2) and (4) and also contrary to others /19/. One reason for this observation may be the dominating right hand part of model B_3:

$$\left(\frac{\partial C_0(t,t')}{\partial t}\right)_{tac} = \frac{0.14}{t \cdot (a/c)^{0.7}} \qquad (15)$$

About 96% of the creep rate calculated according to Eq. (12) depended on the part shown in Eq. (15), which meant that the strength of the concrete had almost no affect on the creep rate. The strength at loading played an important role when estimating the creep /19/. Eq. (14) depended on the age of the HPC being studied and also on the aggregate content, a/c. In order to estimate the affect of aggregate on the measured creep rate in the present study, an extended parameter study was carried out, Figure 10. Symbols in Figure 10 and Table 1:

a denotes aggregate content, Appendix 3 (per mil by volume)
a/c denotes ratio of aggregate to cement (-)
c denotes cement content (kg/m^3)
f_c denotes compressive strength (MPa)
w denotes water content (kg/m^3)
w/c denotes water-cement ratio (-)

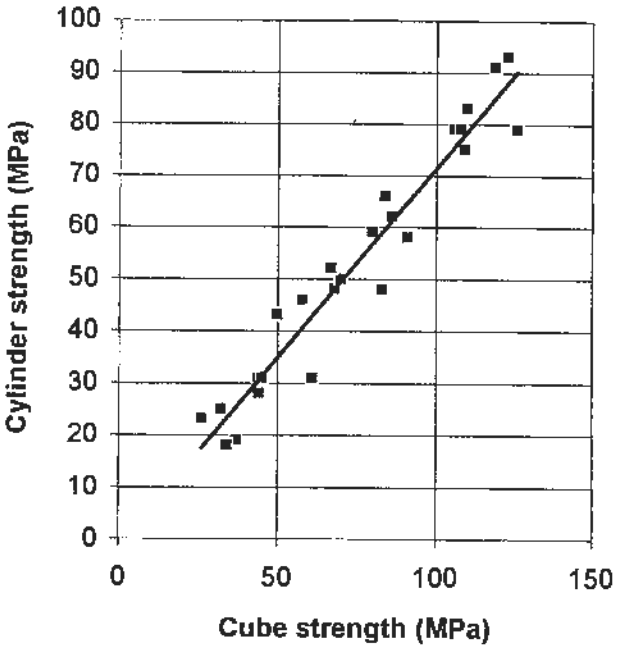

Figure 7. Cylinder strength versus cube strength.

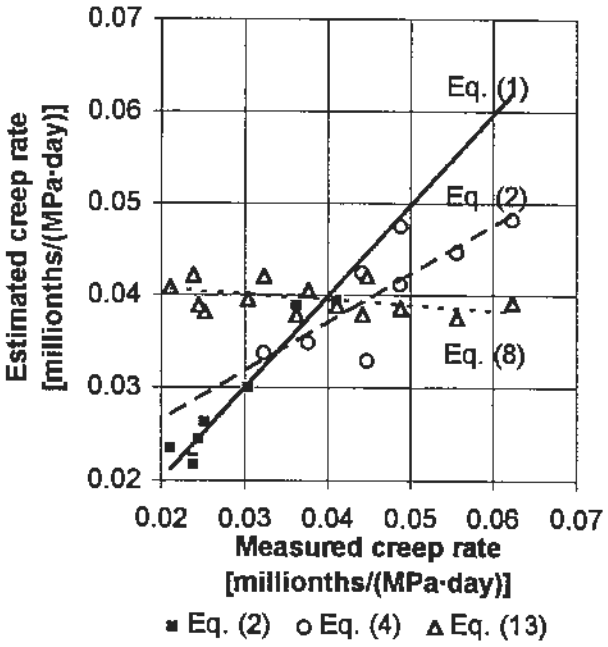

Figure 8. creep rate Estimated according to Eqs. (2), (4) and (13) versus measured creep rate /9/.

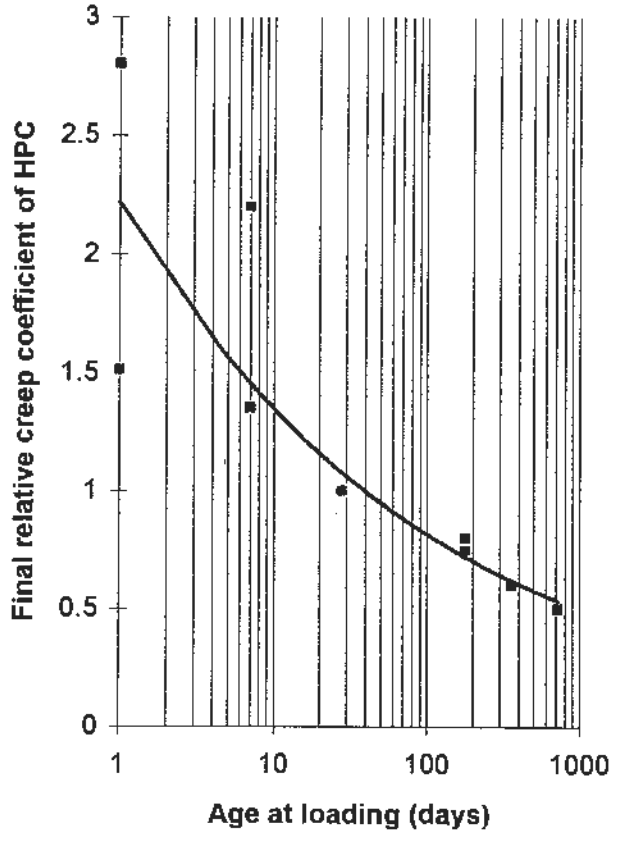

Figure 9. Resulting creep coefficient of HPC versus 28-day relative strength at loading /19/.

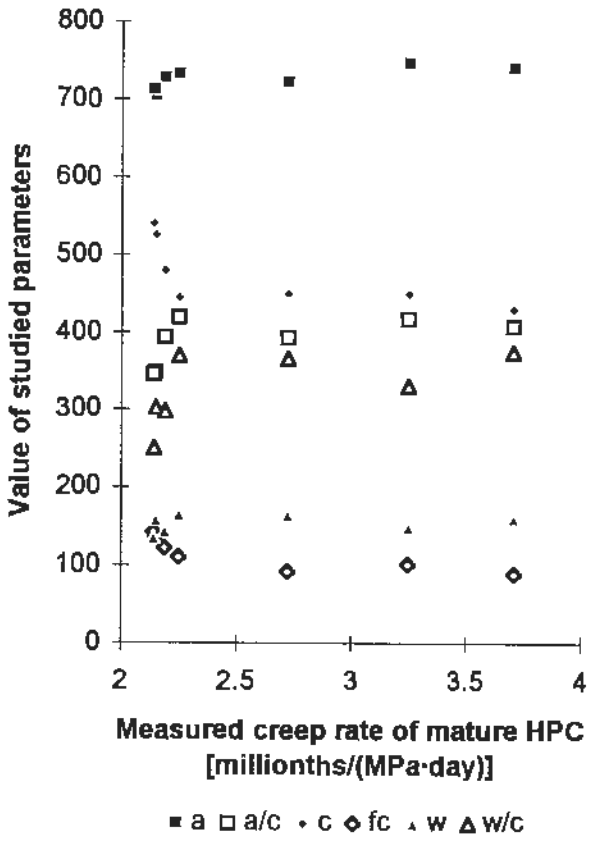

Figure 10. Parameters affecting the creep rate of HPC. Symbols are given below.

Table 1 shows the parameter R^2, Eq. (3) for the creep rate of mature HPC at 210 days' age related to the parameters mentioned above.

Table 1. The parameter R^2 for the creep rate of mature HPC at 210 days' age related to the studied parameters.

Studied parameter	a (per mil by volume)	a/c (-)	c (kg/m^3)	f_c (MPa)	w (kg/m^3)	w/c (-)
R^2	0.62	0.37	0.51	0.66	0.07	0.34

Strength was the most significant parameter related to the creep rate of HPC. After compensation for the content of silica fume the parameter R^2, increased as shown in Eq. (2) and (4). The observation of the elastic modulus in the project according to Eq. (5) was compared to the ACI formula, $E= 57000 \cdot \sqrt{f'_c}$ /15/. Table 3 shows a comparison with a general relationship between elastic modulus and strength /15/.

$$E_t = a \cdot (f_c)^b \qquad (16)$$

a, b denotes constants given in Table 2 (GPa, -)
f_c denotes the cube strength (MPa)
t denotes the time from loading until measurement of deformation (s)
E_t denotes the elastic modulus after t s of loading (GPa)

Table 2 Parameters in Eq. (16)

Formula	Loading time (s)	a (GPa)	b (-)	Parameter R^2
ACI	Unknown	4	0.5	-
Experiments /9/	0.01	5.4	0.46	0.95
	0.1	4.4	0.5	0.94
	1	3.4	0.53	0.92

The comparison between the elastic modulus according to the ACI formula and the results obtained in the experiments underlined the importance of specifying the loading time when obtaining the elastic modulus /1/. The influence of the autogenous shrinkage on the basic creep was shown in Figure 6. No references have been found in the literature. At low stress the effect was large, which may be a problem from the practical point of view (causing cracking, load decrease etc.). Autogenous shrinkage was an important property of HPC but normally negligible for normal concrete /12/.

10. SUMMARY AND CONCLUSIONS

An experimental and numerical study of the basic deformations of HPC was presented. In all about 100 cylinders and 400 cubes of HPC were studied. The following conclusions were drawn:

1) The initial deformation of HPC is mainly dependent on the compressive strength, but also on the method of testing: It was important to specify the time elapsed from loading until measurement of deformations. Otherwise large faults may be obtained in the estimation of the elastic modulus.

2) The long-term creep rate of HPC loaded at young ages is mainly dependent on the maturity at loading.

3) The creep rate of HPC that was mature at loading is dependent on the compressive strength in the mature state.

4) The autogenous shrinkage is related to the development of the internal relative humidity of HPC.

5) The autogenous shrinkage has an affect on the basic creep of HPC, especially at low stresses.

ACKNOWLEDGEMENT

The research was financed by the Norwegian-Swedish Consortium HIGH-PERFORMANCE CONCRETE (BFR, Cementa, Elkem, Scancem Beton, NCC Bygg, NUTEK, SKANSKA and Strängbetong,) which hereby is gratefully acknowledged.

REFERENCES

/1/ P. Acker. Creep and shrinkage of concrete. Proceedings of the Fifth International RILEM Symposium in Barcelona. RILEM. E&FN Spon. London, 7-14 (1993).

/2/ Z. P Bazant, I. Carol. Preliminary guidelines and recommendations for characterising creep and shrinkage in structural design codes. Proceedings of the Fifth International RILEM Symposium in Barcelona. RILEM, E&FN Spon. London, 805-829 (1993).

/3/ E. Tazawa, S. Miyazawa. Autogenous shrinkage of concrete and its importance in concrete technology. Proceedings of the Fifth International RILEM Symposium in Barcelona. RILEM. E&FN Spon. London, 159-168 (1993).

/4/ R le Roy, F de Larrard. Creep and shrinkage of High-Strength Concrete. The Fifth International RILEM Symposium in Barcelona. E&FN Spon. London, 500-508 (1993).

/5/ V Sicard. Origines et propriétés des deformations de retrait et de fluage de bétons à Hautes Performances à partir de 28 heures de durcissement. Laboratoire Matériaux et Durabilité de Constructions. INSA-UPS no 201. Toulouse, 55-81 (1993).

/6/ B. Persson. Self-desiccation and Its Importance in Concrete Technology. Materials and Structures. RILEM. *Accepted for publication (1997).*

/7/ B. Persson. Moisture in concrete after different kinds of curing. Materials and Structures. RILEM. *Accepted for publication (1997).*

/8/ B. Persson. Hydration and strength of High-Performance Concrete. Advanced Cement Based Materials. Elsevier. New York, 3, 107-123 (1996).

/9/ B. Persson. Basic creep of High-Performance Concrete. Report M6:14. CONSORTIUM HIGH-PERFORMANCE CONCRETE. Division of Building Materials. Lund Institute of Technology. University of Lund. Lund, 18-50, 59-73, 88-100, 171-186, 231-235 (1995).

/10/ M. Hassanzadeh. Fracture mechanical properties of High-Performance Concrete. Report M4:05. Consortium HIGH-PERFORMANCE CONCRETE. Division of Building Materials. Lund Institute of Technology. University of Lund. Lund, 9-15 (1994).

/11/ ASTM E 104-85. Standard Practice for Maintaining Constant Relative Humidity by Means of Aqueous Solutions. The American Society for Testing and Materials. Philadelphia, 33-34, 637 (1985).

/12/ Z. P. Bazant. Creep and shrinkage prediction model for analysis and design of concrete structures - model B_3. Materials and Structures. E&FN Spon. London, 28, 357-365 (1995).

/13/ B. Persson. (Early) basic creep of High-Performance Concrete. Fourth International Symposium on the Utilization of High Strength/High Performance Concrete. Presses Ponts et Chaussés. Paris, 405-414 (1996).

/14/ K. Sakata. Prediction of concrete creep and shrinkage. Proceedings of the Fifth International RILEM Symposium in Barcelona. E&FN Spon. London, 649-654 (1993).

/15/ FIP/CEB No. 197. High Strength Concrete. State of the Art Report. Chameleon Press. London, 15-17 (1990).

/16/ J.-P. Jaccoud, A. Leclerq. Some aspects concerning extension of present rules to HPC-structures. Material Properties and Design. Proceedings of the Fourth Weimar Workshop on High Performance Concrete held at Hochschule für Architektur und Bauwesen (HAB). Weimar. Germany, 341-357 (1995).

/17/ O.M. Jensen, P.F. Hansen. Autogenous relative humidity change in silica fume-modified cement paste. Advances in Cement Research. 7, No. 25, 33-38 (1995).

/18/ G. Hedenblad. Personal communication. Division of Building Materials. Lund Institute of Technology. University of Lund. Lund (1996).

/19/ H.S. Müller. Characteristics and Prediction of Creep of High Performance Concrete. Material Properties and Design. Proceedings of the Fourth Weimar Workshop on High Performance Concrete held at Hochschule für Architektur und Bauwesen (HAB). Weimar. Germany, 145-162 (1995).

/20/ B. Persson. Creep of High-Performance Concrete. Report M6:28. CONSORTIUM HIGH-PERFORMANCE CONCRETE. Division of Building Materials. Lund Institute of Technology. University of Lund. Lund, 82-122. *Preliminary (1997).*

Appendix 1.

Chemical composition of cement /9/.

CaO	64.6
Al_2O_3	3.34
Fe_2O_3	4.39
MgO	0.84
K_2O	0.62
Na_2O	0.07
Alkali	0.48
SO_3	2.23
CO_2	0.14
Ignition losses	0.63
Free CaO	1.13
C_2S	22.5
C_3S	53.0
C_3A	1.42
C_4AF	13.4
Blaine fineness	325 m^2/kg
Density	3180 kg/m^3

Appendix 2

Properties of aggregate and silica fume /9, 10/.

Type of aggregate	Elastic modulus	Compressive strength	Split tensile strength	Ignition losses
Quartzite sandstone, Hardeberga (H)	60.2 GPa	332 MPa	15.0 MPa	0.28%
Natural sand, Åstorp (Å)				0.79%
Granite, Norrköping (N)	61.2 GPa	153 MPa	9.6 MPa	1.67%
Pea gravel, Toresta (T)				1.62%
Crushed sand, Bålsta (B)	59.1 GPa	234 MPa	14.3 MPa	1.95%
Granulated silica fume (fineness: 17.5 m^2/g)				2.26%
Silica fume slurry (fineness: 22.5 m^2/g)				1.86%

Appendix 3

Mix design (kg/m^3 dry material) and some properties of the concretes /9/.

Material /Concrete	25g10	29s10	30g10	31g10	33s5	36g10a	37g10	38g5a
Quartzite sandstone, 8-12 mm								460
Quartzite sandstone, 12-16 mm	1060		1005	1020		930	965	460
Natural sand type A, 0-8 mm	750		765	765		790	850	810
Granite, 12-16 mm		1065						
Pea gravel, 8-16 mm					1075			
Natural sand type B, 0-8 mm		770			780			
Cement (Appendix 1)	540	480	525	500	450	450	445	430
Granulated silica fume, s	54		53	50		45	45	22
Silica fume slurry		48			23			
Air-entraining agent (vinsole resin)						0.04		0.02
Superplasticizer (melamine)	9.6	7.8	6.4	4.8	5.3	4.3	5.5	2.8
Water-cement ratio, w/c	0.25	0.30	0.30	0.31	0.33	0.37	0.37	0.38
Air-content (% by total volume)	1.0	0.9	0.9	0.9	0.9	4.5	0.9	4.0
Aggregate content, a	0.734	0.747	0.726	0.734	0.757	0.742	0.752	0.752
Ratio of aggregate to cement, a/c	3.45	3.92	3.47	3.67	4.15	3.92	4.18	4.07
Density (kg/m^3)	2540	2520	2510	2500	2480	2380	2475	2330
Slump (mm)	45	45	230	200	145	170	160	140
28-day cube strength (MPa)	143	122	137	127	101	92	110	89
1-year cube strength (MPa)	162	135	144	139	115	108	124	101
2-year cube strength (MPa)	162	131	149	145	115	121	127	112

Symbols used in Appendix 3:

...g.... denotes granulated silica fume
...s.... denotes silica fume slurry
25..... denotes w/c (%)
.....10 denotes the part of silica fume as calculated on the cement content (%)

Appendix 4

Estimations of the creep rate of HPC according to Eqs. (2), (4) and (13).

Mix design	f'_c	c	w/c	t	t′	t-t′	a/c	B_3-Eq. (13)	B_3-Eq. (13)	k	Eq. (2)	ϖ	Eq. (4)	Ref. /9/
	psi	lb /ft^3	%	days	days	days	-	10^{-10} /psi	10^{-8} /MPa	-	10^{-8} /MPa	-	10^{-8} /MPa	10^{-8} /MPa
38g5a	9200	33	38	210	28	182	4.07	2.68	3.88	0.92	3.94	1	-	4.11
38g5a	9200	33	38	210	2	208	4.07	2.67	3.85	0.92	-	0.54	4.75	4.89
37g10	11300	28	37	210	28	182	4.18	2.63	3.82	1	2.63	1	-	2.52
37g10	11300	28	37	210	2	208	4.18	2.62	3.79	1	-	0.53	4.24	4.42
36g10a	9500	28	37	210	28	182	3.92	2.72	3.95	1	3	1	-	3.04
36g10a	9500	28	37	210	2	208	3.92	2.70	3.92	1	-	0.51	4.82	6.24
33s5	10400	28	33	210	28	182	4.15	2.61	3.78	0.92	3.89	1	-	3.62
33s5	10400	28	33	210	2	208	4.15	2.59	3.75	0.92	-	0.53	4.46	5.56
31g10	13100	31	31	210	28	182	3.67	2.81	4.08	1	2.35	1	-	2.11
31g10	13100	31	31	210	2	208	3.67	2.79	4.05	1	-	0.64	3.48	3.76
30g10	14100	33	30	210	28	182	3.47	2.91	4.21	1	2.24	1	-	2.39
30g10	14100	33	30	210	2	208	3.47	2.89	4.2	1	-	0.65	3.29	4.48
29s10	12600	30	30	210	28	182	39.2	2.69	3.89	1	2.44	1	-	2.45
20s10	12600	30	30	210	2	208	3.92	2.67	3.86	1	-	0.47	4.12	4.88
25g10	14700	34	25	210	28	182	3.45	2.91	4.22	1	2.17	1	-	2.39
25g10	14700	34	25	210	2	208	3.45	2.89	4.2	1	-	0.58	3.37	3.23

Symbols used in Appendix 4:

a denotes the aggregate content (lb/ft^3)
c denotes the cement content [sort: lb/ft^3 related Eq. (8)]
f_{c28} denotes the 28-day cube strength (MPa)
f'_c denotes the 28-day cylinder strength (psi)
k denotes a parameter in Eq. (2) above
t denotes the age of the concrete at estimation of the creep rate (days)
t′ denotes the age of the concrete at loading (days)
w/c denotes the water-cement ratio (%)
B_3 denotes the creep formula given in Eq. (13) above
σ denotes the stress on the concrete
ϖ= σ / f_{c28}